Conditions of applicability of the single-scattering approximation

Michael I. Mishchenko[1*], Li Liu[1] and Gorden Videen[2]

[1]NASA Goddard Institute for Space Studies, 2880 Broadway, New York, NY 10025
[2]US Army Research Laboratory, AMSRD-ARL-CI-EM, 2800 Powder Mill Road, Adelphi, MD 20783-1197
[*]mmishchenko@giss.nasa.gov

Abstract: We employ the numerically exact superposition T-matrix method to perform extensive computations of electromagnetic scattering by small volume elements filled with 8 randomly distributed wavelength-sized spherical particles. The results of these computations are used to examine quantitatively the conditions of applicability of the single-scattering approximation (SSA). We show that one may need large inter-particle distances and low packing densities in order to make the SSA sufficiently accurate.

©2007 Optical Society of America

References and links

1. M. P. Mengüç and S. Manickavasagam, "Characterization of size and structure of agglomerates and inhomogeneous particles via polarized light," Int. J. Eng. Sci. **36**, 1569–1593 (1998).
2. J. W. Hovenier, "Measuring scattering matrices of small particles at optical wavelengths," in *Light Scattering by Nonspherical Particles*, M. I. Mishchenko, J. W. Hovenier, and L. D. Travis, eds. (Academic, San Diego, Calif., 2000), pp. 355–365.
3. H. Volten, O. Muñoz, E. Rol, J. F. de Haan, W. Vassen, J. W. Hovenier, K. Muinonen, and T. Nousiainen, "Scattering matrices of mineral aerosol particles at 441.6 nm and 632.8 nm," J. Geophys. Res. **106**, 17375–17402 (2001).
4. O. Muñoz, H. Volten, H., J. F. de Haan, W. Vassen, and J. W. Hovenier, "Experimental determination of scattering matrices of randomly oriented fly ash and clay particles at 442 and 633 nm," J. Geophys. Res. **106**, 22833–22844 (2001).
5. J. W. Hovenier, H. Volten, O. Muñoz, W. J. van der Zande, and L. B. F. M. Waters, "Laboratory studies of scattering matrices for randomly oriented particles: potentials, problems, and perspectives," J. Quant. Spectrosc. Radiat. Transfer **79/80**, 741–755 (2003).
6. E. Hadamcik, J.-B. Renard, A. C. Levasseur-Regourd, and J. Lasue, "Light scattering by fluffy particles with the PROGRA[2] experiment: mixtures of materials," J. Quant. Spectrosc. Radiat. Transfer **100**, 143–156 (2005).
7. H. Volten, O. Muñoz, J. W. Hovenier, and L. B. F. M. Waters, "An update of the Amsterdam light scattering database," J. Quant. Spectrosc. Radiat. Transfer **100**, 437–443 (2005).
8. Yu. Shkuratov, S. Bondarenko, A. Ovcharenko, C. Pieters, T. Hiroi, H. Volten, O. Muñoz, and G. Videen, "Comparative studies of the reflectance and degree of linear polarization of particulate surfaces and independently scattering particles," J. Quant. Spectrosc. Radiat. Transfer **100**, 340–358 (2006).
9. O. Muñoz, H. Volten, J. W. Hovenier, M. Min, Y. G. Shkuratov, J. P. Jalava, W. J. van der Zande, and L. B. F. M. Waters, "Experimental and computational study of light scattering by irregular particles with extreme refractive indices: hematite and rutile," Astron. Astrophys. **446**, 525–535 (2006).
10. D. Daugeron, J.-B. Renard, P. Personne, G. Brun, and J.-M. André, "Laboratory polarization nephelometer for measurements of optical properties of aerosols," Meas. Sci. Technol. **18**, 632–638 (2007).
11. M. I. Mishchenko, J. W. Hovenier, and D. W. Mackowski, "Single scattering by a small volume element," J. Opt. Soc. Am. A **21**, 71–87 (2004).
12. M. I. Mishchenko, L. D. Travis, and A. A. Lacis, *Multiple Scattering of Light by Particles: Radiative Transfer and Coherent Backscattering* (Cambridge U. Press, Cambridge, UK, 2006).
13. D. W. Mackowski and M. I. Mishchenko, "Calculation of the T matrix and the scattering matrix for ensembles of spheres," J. Opt. Soc. Am. A **13**, 2266–2278 (1996).
14. M. I. Mishchenko, L. D. Travis, and A. A. Lacis, *Scattering, Absorption, and Emission of Light by Small Particles* (Cambridge U. Press, Cambridge, UK, 2002). http://www.giss.nasa.gov/~crmim/books.html.
15. D. Mackowski, K. Fuller, and M. Mishchenko, "Codes for calculation of scattering by clusters of spheres." ftp://ftp.eng.auburn.edu/pub/dmckwski/scatcodes/index.html.

16. M. I. Mishchenko, L. Liu, D. W. Mackowski, B. Cairns, and G. Videen, "Multiple scattering by random particulate media: exact 3D results," Opt. Express **15**, 2822–2836 (2007).
17. M. I. Mishchenko and L. Liu, "Weak localization of electromagnetic waves by densely packed many-particle groups: exact 3D results," J. Quant. Spectrosc. Radiat. Transfer **106**, 616–621 (2007).

1. Introduction

The far-field single-scattering approximation (SSA) is widely used in analyses and interpretation of laboratory measurements of light scattering by tenuous collections of natural and artificial small particles (e.g., [1–10] and references therein). A detailed derivation of the SSA from the exact Foldy–Lax equations has been given in [11, 12]. These publications also provide a qualitative theoretical analysis of the range of applicability of the SSA and a limited numerical illustration based on exact T-matrix results for randomly oriented two-sphere clusters with touching and separated components.

The main objective of this paper is to take advantage of the increased power of scientific workstations in order to extend and render more concrete and quantitative the previous analysis of the range of applicability of the SSA. Specifically, we apply the superposition T-matrix method (STMM) [13–15] to a small volume element filled with eight randomly distributed wavelength-sized particles. By keeping the size of the particles fixed and increasing the average interparticle separation, we illustrate the gradual disappearance of various multiple-scattering effects and the onset of the single-scattering regime. These results provide a direct quantitative estimate of what inter-particle separation is necessary in order to make the SSA accurate to within a prescribed numerical margin.

In order to avoid redundancy and save space, we take advantage of the on-line availability of [14] and use exactly the same terminology and notation.

2. Numerical results

As shown in Fig. 1, we assume that eight identical spherical particles are distributed randomly throughout a spherical volume with a radius R much greater than the particle radius r. The size parameter of the particles is fixed at $k_1 r = 4$, where k_1 is the wave number in the surrounding medium; whereas, the size parameter of the spherical volume is varied from $k_1 R = 12$ to $k_1 R = 72$ in steps of 6. This procedure yields particle volume concentrations ρ ranging from 29.6% down to 0.14%. The relative refractive index of the particles is fixed at 1.32.

The arrangement of the eight particles inside the $k_1 R = 12$ volume is random but such that each particle is in contact with at least one other particle. The other ten particulate volumes with $k_1 R = 18, 24, …, 72$ are obtained by uniformly scaling all particle coordinates of the $k_1 R = 12$ volume while keeping the size of the particles fixed. This procedure is illustrated in Fig. 1, which shows the original $k_1 R = 12$ volume element and the derivative $k_1 R = 24$ volume element.

$k_1 R = 24$

$k_1 R = 12$
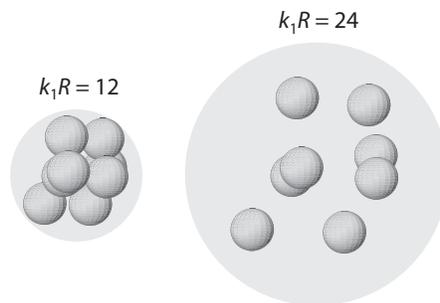
Fig. 1. Spherical volume elements filled with eight randomly positioned, identical particles.
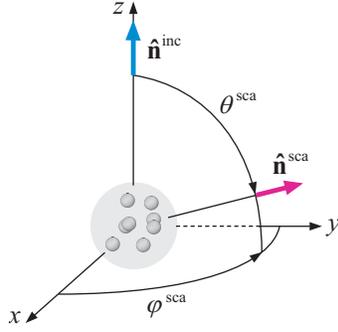
Fig. 2. Electromagnetic scattering by a small volume element.

To simulate light scattering by a statistically random volume element, one needs an efficient way of averaging the computed scattering properties over very many different configurations of a multi-particle group. The approach adopted for this study is to use only one randomly configured 8-particle group and average over all possible orientations of this configuration with respect to the laboratory coordinate system [16]. This procedure yields in effect an infinite continuous set of random realizations of the 8-particle group and enables one to take full advantage of the highly efficient semi-analytical orientation averaging technique afforded by the STMM [14, 15].

We assume that the statistically random volume element is illuminated by a plane electromagnetic wave or a parallel quasi-monochromatic beam of light propagating in the direction $\hat{\mathbf{n}}^{\text{inc}}$ (Fig. 2). The observation direction is specified by the unit vector $\hat{\mathbf{n}}^{\text{sca}}$. Since all scattering properties are averaged over the uniform orientation distribution of a multi-particle group, we can simplify the discussion by assuming that the incidence direction coincides with the positive direction of the z-axis of the laboratory reference frame and that $\varphi^{\text{sca}} = 0$. Then the scattering direction can be uniquely characterized by the scattering angle $\Theta = \theta^{\text{sca}}$ and the transformation of the Stokes parameters of the incident light into those of the light scattered in the observation direction can be written in terms of the so-called normalized Stokes scattering matrix [14]:

$$
\begin{bmatrix} I^{\text{sca}} \\ Q^{\text{sca}} \\ U^{\text{sca}} \\ V^{\text{sca}} \end{bmatrix} \propto \begin{bmatrix} a_1(\Theta) & b_1(\Theta) & 0 & 0 \\ b_1(\Theta) & a_2(\Theta) & 0 & 0 \\ 0 & 0 & a_3(\Theta) & b_2(\Theta) \\ 0 & 0 & -b_2(\Theta) & a_4(\Theta) \end{bmatrix} \begin{bmatrix} I^{\text{inc}} \\ Q^{\text{inc}} \\ U^{\text{inc}} \\ V^{\text{inc}} \end{bmatrix}.
\tag{1}
$$

The specific block-diagonal structure of the scattering matrix is confirmed by the T-matrix results: all scattering matrix elements denoted in Eq. (1) by a zero have been found to be at least an order of magnitude smaller than the smallest non-zero element (in the absolute-value sense). The (1,1) element, called the phase function, is normalized according to

$$
\frac{1}{2} \int_0^\pi d\Theta \sin\Theta \, a_1(\Theta) = 1.
\tag{2}
$$

The results of our extensive T-matrix computations are summarized in Figs. 3–5. Figure 3 depicts the dimensionless extinction cross section ratio defined as

$$
\frac{C_{\text{ext}}(\text{volume element})}{8\,C_{\text{ext}}(\text{one particle})}
\tag{3}
$$
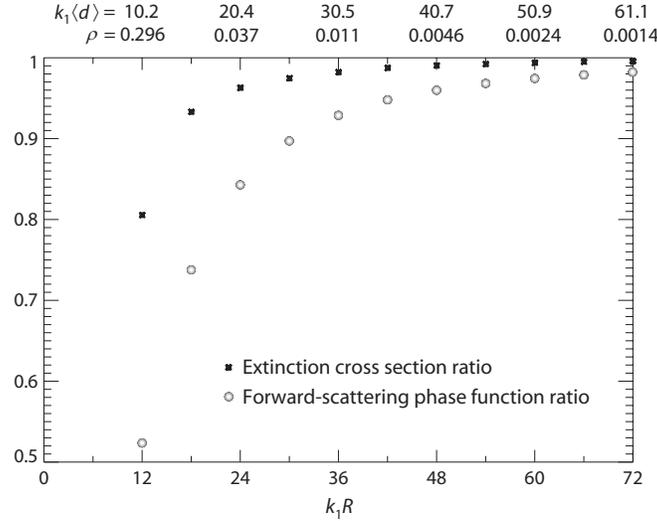
Fig. 3. Ratios defined by Eqs. (3) and (4). Also shown are the ρ and $k_1\langle d \rangle$ values corresponding to $k_1 R = 12, 24, 36, 48, 60,$ and 72.

and the forward-scattering phase function ratio defined as

$$\frac{a_1(\Theta = 0°, \text{ volume element})}{8\,a_1(\Theta = 0°, \text{ one particle})}. \tag{4}$$

This figure also quantifies the particle volume concentration (or packing density) ρ and the quantity $k_1\langle d \rangle$ as functions of $k_1 R$, where $\langle d \rangle$ is the average distance between the sphere centers. Figure 4 shows the phase function and the ratios of the non-zero Stokes scattering matrix elements to the phase function for the various volume elements as well as for a single sphere. Figure 5 details the phase functions at forward and near-forward scattering directions as well as depicts the quantity

$$\tfrac{1}{2}[a_1(\Theta) - a_2(\Theta)]. \tag{5}$$

The latter describes the angular distribution of the cross-polarized scattered intensity provided that the incident light is fully linearly polarized in the xz plane.

3. Discussion

The gist of the SSA is that one can neglect the response of each particle in a volume element to the fields scattered by all the other particles and assume that each particle is excited only by the external incident field. For the SSA to be applicable, the volume element must be optically thin and the inter-particle separation must be sufficiently large. The threshold optical thickness value for widely separated particles can be determined using an approximate approach based on the radiative transfer theory [12]. However, exact computations of electromagnetic scattering such as those presented in Figs. 3–5 are needed to determine the requisite minimal inter-particle distance.

According to the simple SSA [11, 12], the extinction cross section ratio defined by Eq. (3) must be equal to one. Furthermore, according to the modified uncorrelated SSA (MUSSA), the elements of the normalized Stokes scattering matrix for a volume element must be equal to those for a single sphere. Figures 3 and 4 demonstrate the departure from these requisite values for different packing densities. They show that the particle packing density should be smaller than 1% and $k_1\langle d \rangle$ should be greater than 30 for the SSA for there to be negligible
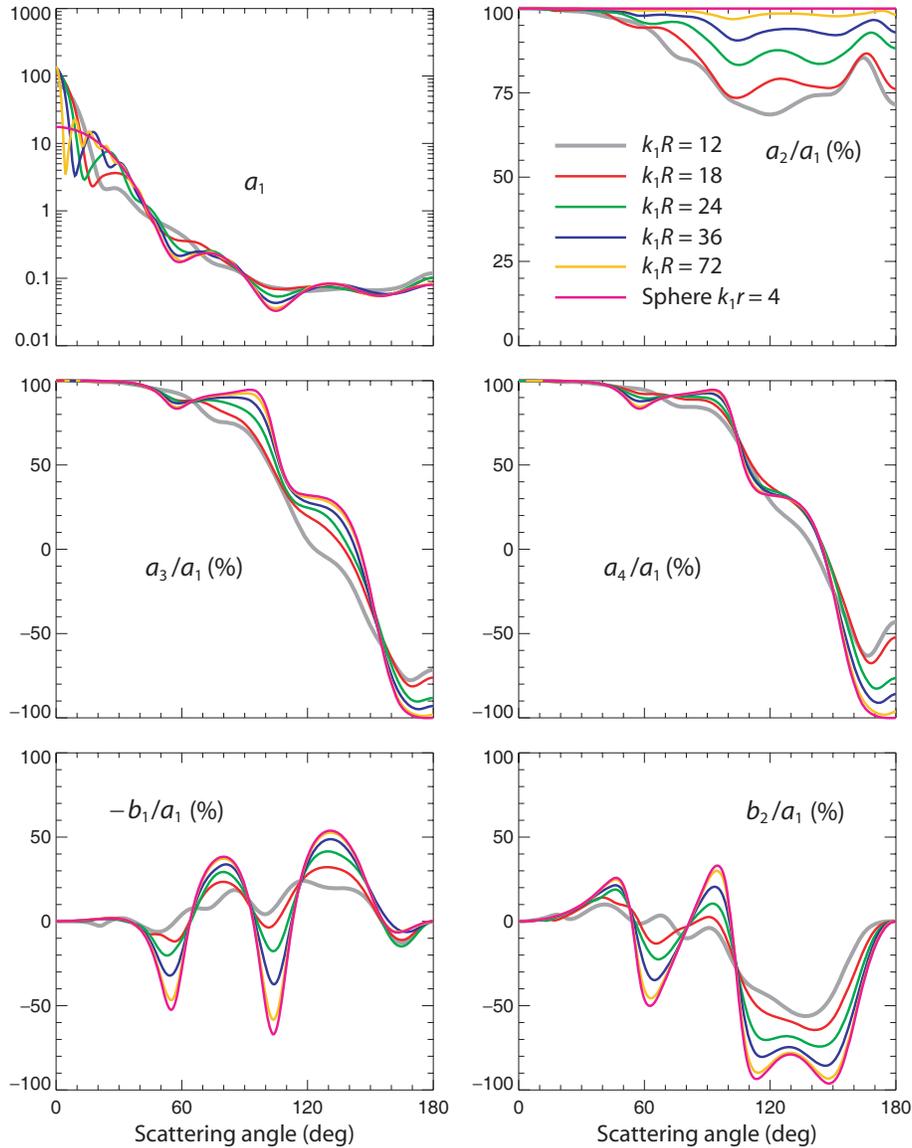
Fig. 4. Elements of the normalized Stokes scattering matrix.

differences when using the SSA.

While quite large separations are needed for the accuracy of the SSA to be within a few percent, the applicability of the SSA ultimately depends on the applications and required tolerances. For many particle characterization applications such tolerances are requisite, but for other applications, the tolerances may be more relaxed. For example, the ratios $-b_1/a_1$ and b_2/a_1 tend to retain the basic features of the single spherical particle to rather large packing densities. For these ratios, the frequency of angular oscillations remains predominantly the same, but the amplitude of oscillations decreases with increasing packing density until the largest density is reached, in which case the scattering properties no longer retain the obvious single-particle features. The retention of the single-particle frequencies for relatively large densities may potentially be used to size the individual particles in this cluster from these Stokes-matrix element ratios. In this application the tolerance of the SSA appears relatively
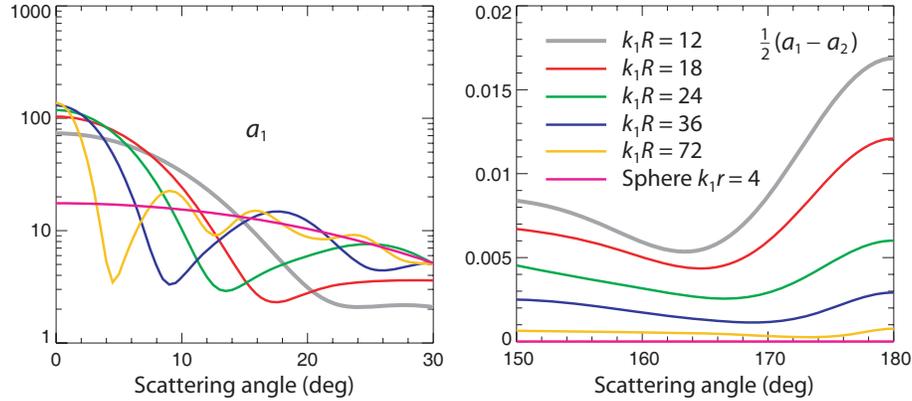
Fig. 5. Forward-scattering phase function and the quantity $\frac{1}{2}[a_1(\Theta) - a_2(\Theta)]$.

relaxed.

An important effect caused by multiple scattering is coherent backscattering (or weak localization of electromagnetic waves) [16, 17]. This effect can be exhibited especially clearly by the quantity defined by Eq. (5) since the cross-polarized scattered intensity is identically equal to zero for a single spherical particle. The right-hand panel of Fig. 5 shows that the backscattering peak has the largest amplitude and width for $k_1R = 12$. With increasing inter-particle separation, the amplitude and the width of the peak decrease, thereby corroborating the multiple-scattering origin and the interference nature of coherent backscattering. Obviously, it takes very low particle packing densities to fully extinguish this effect.

A fundamental single-scattering phenomenon exhibited by multi-particle groups is the forward-scattering interference illustrated by the left-hand panel of Fig. 5 and discussed in detail in [11, 12, 16]. For widely separated particles, the ratio defined by Eq. (4) must be equal to one. However, Fig. 3 shows that this ratio approaches the asymptotic value of one with increasing k_1R even slower than the extinction cross section ratio. The angular width of the forward-scattering interference peak is inversely proportional to $k_1\langle d \rangle$. Figure 5 obviously indicates that $k_1\langle d \rangle$ must be much greater than 60 in order to ensure that the interference peak is narrow enough and does not affect the interpretation of laboratory measurements in terms of the MUSSA.

4. Conclusion

Our numerically exact T-matrix results demonstrate that one may need large inter-particle distances and low packing densities in order to make the SSA sufficiently accurate for groups of wavelength-sized particles. This implies that one should exercise caution when interpreting laboratory data such as those presented in [1–10].

Obviously, more work still needs to be done in order to extend our analysis to groups consisting of larger and possibly polydisperse particles. The rapidly increasing efficiency of scientific workstations should make this extension feasible in the very near future.

Acknowledgments